



## OPEN

## SUBJECT AREAS:

BASAL GANGLIA

SOCIAL BEHAVIOUR

EXTRACELLULAR RECORDING

# A wireless neural recording system with a precision motorized microdrive for freely behaving animals

Taku Hasegawa<sup>1,2,3</sup>, Hisataka Fujimoto<sup>2,4</sup>, Koichiro Tashiro<sup>1</sup>, Mayu Nonomura<sup>1</sup>, Akira Tsuchiya<sup>5</sup> & Dai Watanabe<sup>1,2</sup>

Received

28 August 2014

Accepted

16 December 2014

Published

19 January 2015

Correspondence and requests for materials should be addressed to D.W. (dai@phy.med.kyoto-u.ac.jp)

<sup>1</sup>Department of Biological Sciences, Graduate School of Medicine, Kyoto University, Kyoto, Japan, <sup>2</sup>Department of Molecular and Systems Biology, Graduate School of Biostudies, Kyoto University, Kyoto, Japan, <sup>3</sup>Training Program of Leaders for Integrated Medical System for Fruitful Healthy-Longevity Society, Center for the Promotion of Interdisciplinary Education and Research, Kyoto University, Kyoto, Japan, <sup>4</sup>Department of Developmental Molecular Anatomy, Graduate School of Medical Sciences, Kyushu University, Fukuoka, Japan, <sup>5</sup>Department of Communications and Computer Engineering, Graduate School of Informatics, Kyoto University, Kyoto, Japan.

The brain is composed of many different types of neurons. Therefore, analysis of brain activity with single-cell resolution could provide fundamental insights into brain mechanisms. However, the electrical signal of an individual neuron is very small, and precise isolation of single neuronal activity from moving subjects is still challenging. To measure single-unit signals in actively behaving states, establishment of technologies that enable fine control of electrode positioning and strict spike sorting is essential. To further apply such a single-cell recording approach to small brain areas in naturally behaving animals in large spaces or during social interaction, we developed a compact wireless recording system with a motorized microdrive. Wireless control of electrode placement facilitates the exploration of single neuronal activity without affecting animal behaviors. Because the system is equipped with a newly developed data-encoding program, the recorded data are readily compressed almost to theoretical limits and securely transmitted to a host computer. Brain activity can thereby be stably monitored in real time and further analyzed using online or offline spike sorting. Our wireless recording approach using a precision motorized microdrive will become a powerful tool for studying brain mechanisms underlying natural or social behaviors.

The brain is a highly organized structure consisting of many different types of neurons, which transmit information through their electrical activity, termed “spikes” or “action potentials”. Therefore, studies of such electrical signals at single-cell resolution can provide valuable insights into brain functions<sup>1,2</sup>. However, because extracellularly detected electrical signals of individual neurons are very faint, precise isolation of single neuronal activity from background noise and other neuronal activity becomes a key technical challenge, especially in studies using freely behaving animals. To overcome this difficulty, various electrophysiological methods have been reported<sup>3–6</sup>. Although the configurations of electrodes and recording devices vary depending on the target brain areas or behaviors, technical efforts for measuring single neuronal activity can be lumped into two major approaches: electrode positioning and spike sorting<sup>7–10</sup>. The former approach emphasizes careful manipulation of recording electrodes to position them close to target cells. The latter approach is primarily based on the presumed consistency of the spike shape and amplitude for a given neuron, and enables recorded spikes to be sorted and classified into spike clusters of different putative neurons.

For measuring neuronal activity in relatively small brain areas such as the vocal-related nuclei in songbirds and the accessory olfactory bulb in rodents, compact and lightweight motorized microdrive devices have been developed<sup>8,11–13</sup>. These miniature microdrives are equipped with small brushless DC motors (BLDCs) for the electrode positioning, and are connected through cables with an electrophysiological amplifier and a motor driver for the BLDCs<sup>8,11–13</sup>. Because the position of the electrodes can be remotely controlled without interfering with animal behaviors<sup>8</sup>, neuronal activity related to naturally occurring behaviors can be efficiently explored, and can often successfully be isolated at single cell resolution<sup>8</sup>. Furthermore, by applying spike sorting to the recorded data, more precise analyses of single neuronal activity can be achieved. Indeed, this technology has greatly contributed to the understanding of neural mechanisms underlying vocal communication in songbirds<sup>11,13–15</sup>



and pheromonal communication in rodents<sup>12</sup>. With further modifications of such motorized microdrive systems, precise electrophysiological analyses at the single-cell level could be applied to other behavioral studies.

To meet the strong demands for the understanding of brain circuit operations in freely behaving animals in larger spaces or natural environments, different types of wireless recording devices have been developed<sup>16–23</sup> and are expanding the range of behaviors that can be studied. Similarly, if neural recording using precision motorized microdrives could be performed without cables, the motorized microdrive system would also be useful to investigate single neuronal activity from freely behaving animals in broader spaces, in either indoor or outdoor settings. The main challenge in developing such a wireless recording system with a motorized microdrive is that all of the component devices, including the motor driver and an electrophysiological amplifier, must be built into a compact and lightweight package that a subject animal can carry with minimal discomfort or hindrance.

In this study, we report a novel wireless recording system with a motorized microdrive. For this, we have developed a compact wireless interface (WIF) and improved the “wired” recording system into a compact and handy “wireless” one. The WIF includes a motor driver for BLDCs and an electrophysiological amplifier in addition to a Bluetooth wireless transceiver. Thus, the electrode position can be wirelessly controlled to isolate single neuronal activity in naturally behaving animals without interfering with their behaviors. Because the WIF is equipped with a newly developed data-encoding program optimized for neural signals, the brain activity can be continuously observed in real time and further analyzed using online or offline spike-sorting programs. To assess the utility of the wireless recording system with motorized microdrive, we performed single unit recording in the thalamic parafascicular nucleus (PF)<sup>24–26</sup> in a naturally behaving rat, and observed that a PF neuron increased its firing rate at the moment of encounter with a conspecific, and the neuron maintained the firing rate during the social interaction. Our wireless recording using a precision motorized microdrive will become a useful tool with broad applicability for exploring brain mechanisms underlying natural or social behaviors.

## Results

**A motor driver and a wireless interface construct.** We first designed a miniature motor driver to operate a motorized microdrive (Fig. 1a, Supplementary Fig. S1). As previously described<sup>13</sup>, the microdrive includes three planetary-gear BLDCs to move three recording electrodes forward and backward along the motor axis. Each BLDC has three terminals, which are internally connected with different electro-magnetic windings (Fig. 1b, left). To precisely control the position of the three electrodes in an independent manner, the motor driver must supply appropriate sets of command signals to all these nine BLDC terminals.

To make the motor driver compact, we reduced the total number of the command signals for motor control and, as previously reported<sup>8</sup>, adopted combinations of only five voltage patterns to control all the BLDCs. As illustrated in the left panel of Figure 1b, each BLDC was connected to receive a unique command voltage signal (Va1, Va2, or Va3) in addition to common ones (Vb and Vc). When the motor driver generates a square voltage wave in Va1 with a 90° phase difference to the common square wave in Vb, and simultaneously supplies constant voltages to Va2 and Va3, the electromagnetic force for motor rotation is only produced in motor 1, and not in motor 2 or 3 (Fig. 1b right). The travel distance of the electrode is controlled by changing the number of square pulses (N in Fig. 1b). The direction of the electrode movement can be reversed by opposing the phase difference between these two square waves. In this way, we can discretely control the three BLDCs. Such motor control using square voltage waves is advant-

ageous in developing a small and lightweight motor driver; desired square voltage waveforms with sufficient currents to drive the BLDCs (approximately 100 mA) can be easily synthesized, simply by operating analogue switches through the programmable input/output ports (GPIOs) of a microcontroller (MCU) (Fig. 1c).

For the isolation of single neuronal activity, micrometer-scale control of electrode position often becomes essential. Because the motor control is open-loop, the initial positional relationship between the stator windings and the magnet rotor in the BLDCs cannot be controlled. This may affect the motor movement especially when applying a small number of square voltage pulses. To test whether our motor driver can actually adjust the electrode position with micrometer resolution, we estimated the minimal step distance of the electrode movement. The motor driver was connected to a microdrive, and command voltage signals consisting of 1 to 24 square pulses were generated. When command signals of less than 5 square pulses were applied, the BLDC movement became unstable. In contrast, when 5 or more square pulses were applied as the command signal, the average displacement of the electrode tip linearly increased as a function of the pulse number (displacement (μm) = 0.34N – 0.54 with R<sup>2</sup> = 0.997, where N (≥ 5) is the number of square pulses) (Fig. 1d). Thus the practical minimal step distance can be given by a command signal of 5 square pulses, which results in approximately 1.2 μm of electrode movement. This indicates that our motor driver, simply consisting of a MCU and analogue switches, can achieve precision control of electrode position with micrometer resolution.

Next we constructed an all-in-one wireless interface (WIF) that includes all of the functions required for wireless recording in addition to a motor driver (Fig. 1e). Because the MCU, used for operation of our motor driver, also contains useful functions for communication with and operation of other devices, we utilized these MCU-embedded functions (see Methods) and also integrated an electrophysiological amplifier and a Bluetooth wireless transceiver into a compact circuit board (Fig. 1e and f). As a result, we could make the WIF compact enough (16 (w) × 20 (h) × 7 (d) mm, 3.1 g) to be mountable on the animal head along with the motorized microdrive (Fig. 1g). Within one week after implantation of the wireless recording system, the animals carrying the whole system, including a harness with a 16 g battery pack, could perform a complex operant task at the same level as before surgery (Supplementary Fig. S2). Thus our wireless recording system is sufficiently small and lightweight to study complex animal behavior, and it enables the precise control of electrode movement without affecting animal behaviors.

**Data compression for stable wireless transmission.** For precise single unit analysis, the neuronal signals must be continuously monitored in real time to control electrode placement or to perform spike-sorting analysis. In our system, recorded neuronal signals are converted to digital data with a sampling frequency of 20 kHz and a 10-bit resolution by an analog-to-digital converter (ADC) (Fig. 2a upper). If the digitized data are encoded to a 10-bit length as they are, the wireless transceiver must continuously transmit the data at 200 kilobits per second (kbps) or faster. To address whether, and how far, our wireless recording system can stably transmit at the required bit rate, we examined the actual data transfer rate in our laboratory space. The average transfer rate gradually decreased with increasing distance, and was reduced to less than 200 kbps approximately 5 m from the WIF (Fig. 2b). Furthermore, the movement of the WIF greatly affected its transfer rate and the wireless transmission became unstable.

To expand the range of stable wireless communication, we developed a data-encoding program that converts sampled values into variable bit-length codes to reduce the data size. In extracellular recording of neuronal signals, although “spike” events display large deviation from the basal resting potential, a considerable proportion

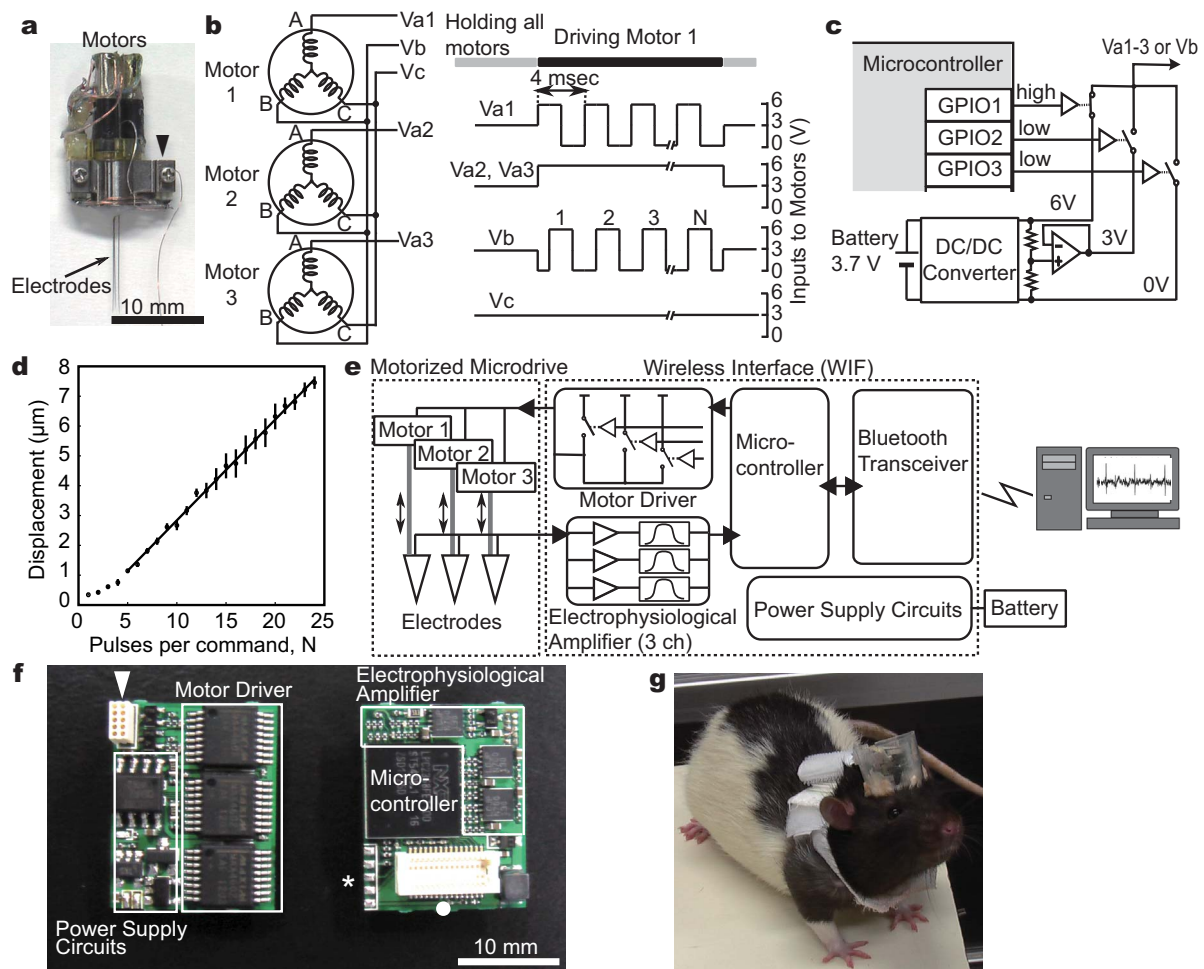


**Figure 1** | A wireless interface (WIF) for the motorized microdrive. (a) A motorized microdrive with three recording electrodes. Electrodes and BLDCs are connected to the WIF through a small 10-pin connector (arrow head). (b) A wiring schematic between the BLDCs and the motor driver (left). An example set of the motor driver command for driving motor 1 (right). (c) A circuit diagram of the motor driver. Square voltage waves are synthesized by operation of three analog switches through the programmable input/output ports (GPIOs) in the microcontroller (MCU). (d) Precision control of the electrode movements by square voltage pulses. The average displacement of an electrode linearly increases as a function of the number of pulses when 5 or more square pulses are applied as the command signal. Error bars indicate  $\pm$  s.e.m. ( $n = 10$ ). (e) System overview. An electrophysiological amplifier, consisting of amplifier and filter circuits, is connected with the analog-to-digital converter (ADC) of the MCU, which converts analog recorded signals into digital data; a Bluetooth wireless transceiver is connected with the universal asynchronous receiver transmitter (UART) port of the MCU. (f) A circuit board of the WIF (both sides). An arrowhead, a closed circle, and an asterisk indicate a connector for the motorized microdrive, a connector for the Bluetooth transceiver, and the terminals for updating the firmware of the MCU, respectively. (g) A rat carrying a microdrive and WIF on the head, and a battery on the back.

of data points are concentrated around the basal level because spikes are brief events (Supplementary Fig. S3), meaning that values of higher bits tend to be zero and non-informative. Therefore, to reduce bit lengths, after analog-to-digital conversion, we added an encoding process (Fig. 2a middle) that removes consecutive zeros from the binary strings and instead adds strings indicating the bit length of the informative part. As shown in Figure 2c, each sampled value (u) can be expressed with a sign bit (S), consecutive zeros, and informative n-bit string (n is defined as an integer satisfying  $2^n > |u|$ ). On the other hand, after the variable-length encoding process, each data point is expressed as a variable-length string consisting of unary representation for the informative bit length ( $n-k+1$ ; k is a compression-parameter integer satisfying  $0 \leq k \leq n$ , and can be remotely controlled) and binary representation for the sign and informative value (Fig. 2c).

To evaluate the compression efficiency, the data size of neural recordings in the cortex, hippocampus, or thalamus ( $n = 6$  each) was compared before and after the variable-length encoding process. In most cases, the encoding process effectively reduced the sampled

data (Fig. 2d, compression efficiency: cortex  $59.6 \pm 12.2\%$ ; hippocampus  $68.3 \pm 10.2\%$ ; and thalamus  $71.4 \pm 15.5\%$  (mean  $\pm$  s.d.,  $n = 6$  each)). Thus the variable-length encoding process reduced the minimal transfer rate required for real-time data transmission to  $132.8 \pm 26.2$  kbps (blue line in Fig. 2b). However, when the sampled neuronal signal frequently reached a high value, for example when spikes were generated with high frequency (asterisk in Fig. 2d), the total data size after the variable-length encoding process became rather larger than that of the original data encoded with a fixed-length binary coding. To compensate for this, we added the first-order difference operation before the variable-length encoding process (Fig. 2a bottom), because the first-order difference operation can effectively cancel out a large deviation from zero and reduce the sampled value even when generating action potentials (Supplementary Fig. S3). As a result, the variable-length encoding process with the first-order difference operation consistently rendered the data size smaller not only in comparison with the original but also in comparison with the encoding process only (Supplementary Fig. S4, Fig. 2d). Remarkably, through optimizing the variable-length

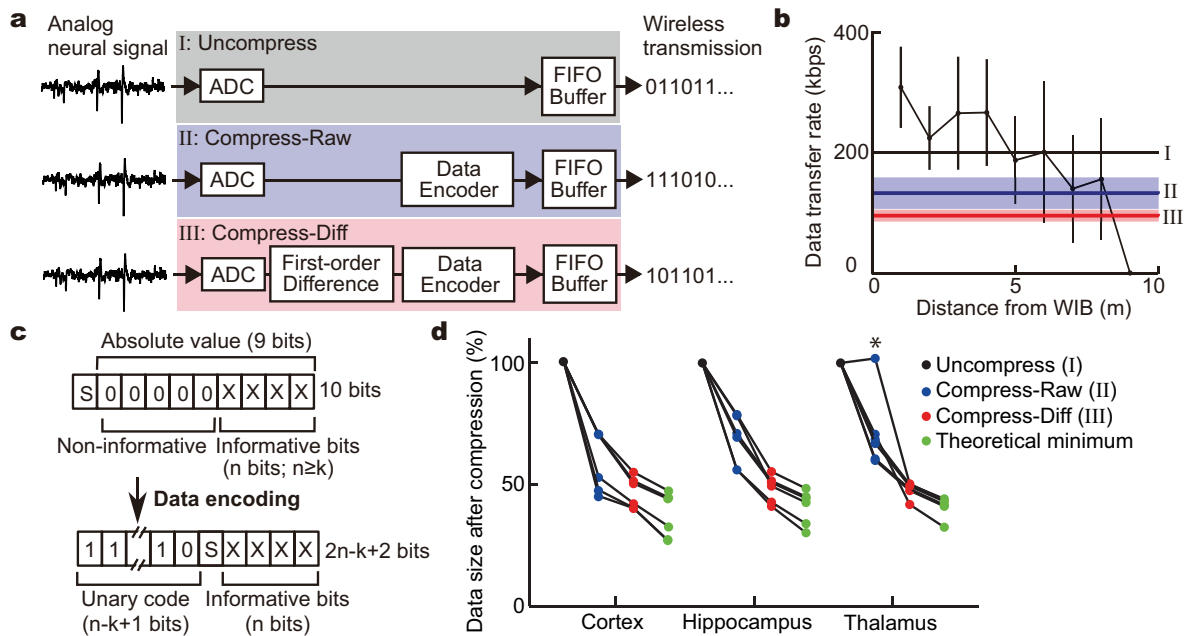


**Figure 2 | Data compression for stable wireless transmission.** (a) Schematics for signal processing of the recorded neuronal signals in the MCU. ADC, analog-to-digital converter; FIFO Buffer, first-in first-out ring buffer; Data Encoder, variable-length encoding process; First-order Difference, first-order difference operation. (b) The relationship between the data transfer rate and the distance. Thick horizontal black, blue, and red lines indicate the transfer rates required for real-time data transmission of neural signals with a fixed-length format (I), variable-length encoding process only (II), and first-order difference operation and variable-encoding process (III), respectively. Pale blue and red bands indicate s.d. in (II) and (III), respectively. (c) Data format before and after the variable-length encoding process. (d) Comparison of compression efficiency. Data size of the neuronal activity with a high firing rate (asterisk) became larger after the variable-length encoding process than the original. Note that the data could be compressed almost to the theoretical minimum size calculated by Shannon entropy.

encoder by adjusting the value of compression-parameter  $k$  after the first-order difference operation, the individual data sizes were reduced nearly to their theoretical limit for lossless compression, which could be calculated as Shannon entropy<sup>27</sup> (Fig. 2d). Thus, our data-encoding program effectively reduces the minimal transfer rate required for real-time data transmission to  $95.3 \pm 9.9$  kbps (red line in Fig. 2b), and successfully expands the wireless communication range, where neural activity can be stably monitored in real time.

**Signal quality of the wireless recording system.** To evaluate the signal quality of the wireless system, we compared the recorded data of our WIB with those of a conventional wired recording system. To make a direct comparison between wireless and wired recording systems, the same recording electrodes were connected to both the WIB and the conventional electrophysiological amplifier in a parallel manner, and we simultaneously performed wireless and wired recordings in the cortex, hippocampus, or thalamus of head-fixed rats.

The signal amplitude and the level of background noise were almost equivalent between these two systems (Fig. 3a). Similar to the spikes obtained using the wired system, the wirelessly-recorded spikes, detected by amplitude thresholding and isolated by spike shapes, were clearly distinguished from the background noise (Fig. 3b). The signal-to-noise ratio (SNR) (average SNR in the wireless and wired system: 21.85 dB and 22.13 dB, respectively) was closely similar between these two systems (Fig. 3c) (Pearson's correlation coefficient = 0.9925,  $n = 11$ ). Furthermore, the patterns of spike clusters were almost the same (Fig. 3b and Supplementary Fig. S5), and the numbers of detected spike events in each recording session were completely identical between these two different recording configurations. Thus, the direct comparison between wireless and wired recording systems demonstrated that wireless electrophysiological recording using our WIB can provide recording quality

of neural signals comparable to the conventional wired electrophysiological amplifier.

**Wireless recording in freely behaving animals using the motorized microdrive system.** Encounters with and recognition of familiar conspecifics induce characteristic behaviors. However, neural processing of such social-cognitive interactions is largely undefined. We conducted a trial of our wireless recording system to explore neuronal activity relevant to social contact. The motorized microdrive was implanted so as to target the thalamic parafascicular nucleus (PF) (Fig. 4a), which is known to be a part of the ascending reticular activating system<sup>28</sup>, and the WIB was mounted on the rat's head along with the microdrive. After the subject equipped with the wireless recording system was released in an 80 cm  $\times$  80 cm square space, we wirelessly observed the neural activity in real time to adjust the electrode placement. When faint signals of spike discharges were detected (Fig. 4b left), by carefully advancing the recording electrode, the peak-to-peak amplitudes of spike events ( $V_{pp}$ ) became larger, presumably reflecting the approach of the electrode tip to the cell body of the PF neuron (Fig. 4b middle and right). Thus we could efficiently isolate spikes of the PF neurons from the background noise by wirelessly adjusting the electrode position, indicating that, similar to the tethered motorized microdrive, our wireless system allows high-quality recording and analysis of single neuronal activity in behaving animals.

Previous studies demonstrated that the PF neurons, which extensively project to the cortex and the basal ganglia, display activity in response to salient stimuli, suggesting that they may play an important role in selecting or supporting complex forms of cognition and voluntary behavior depending on the situations<sup>24,29,30</sup>. To test whether the PF neurons alter their activity depending on the social situations, we introduced another rat, which was familiar to the subject, in the same field (Fig. 4c). As shown in Figure 4d, the PF

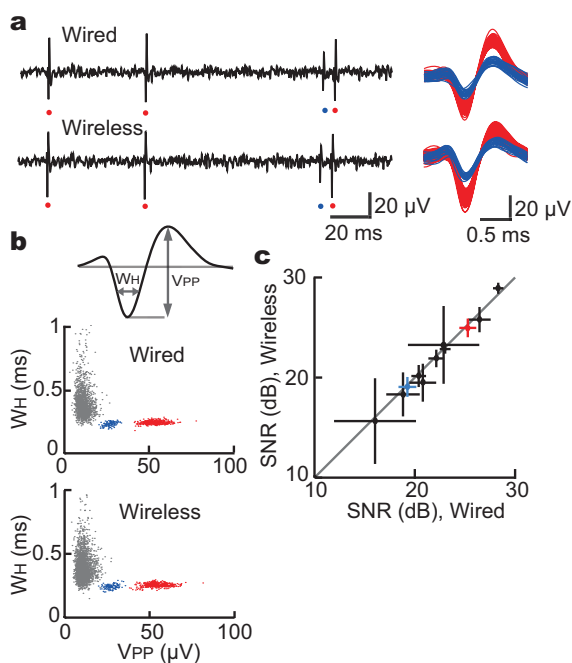


**Figure 3 | Direct comparison of signal quality between wired and wireless systems.** (a) Neural data from the same electrode obtained simultaneously using wired and wireless systems. The example trace included spikes with two different amplitudes (red and blue), suggesting that activities of two different neurons were detected. (b) Scatter plot of spike width ( $W_H$ ) and spike peak amplitude ( $V_{PP}$ ) was generated for the same data presented in (a). All deflections with negative peaks below  $-6 \mu\text{V}$ , including background noise (grey), were used. (c) Comparison of signal-to-noise ratio (SNR, mean  $\pm$  s.d.) in each single unit activity between the wired and wireless systems ( $n = 11$ ; Pearson's correlation coefficient = 0.9925).

neuron increased its firing rate in response to the encounter with the conspecific animal. Interestingly, the neuron maintained the increased firing rate while the second animal was present in the same space, possibly affecting the behavioral bias during the social contact.

Finally, to estimate the practical transmission range of the WIF implanted on a behaving subject, we performed wireless recording in an indoor open space (Fig. 5). Because the space was not equipped with an electric power socket, a battery-operated laptop computer with a compact Bluetooth transceiver was used for all the recording tasks: controlling the electrode placement, decoding the compressed recorded data, and monitoring single neuronal activity in real time. When the animal was placed more than 8 m from the computer, the wireless transmission was frequently interrupted by a slight movement of the subject. However, at a distance less than 5 m from the computer, the neuronal signals could be stably observed during various behaviors. Importantly, although the space was not electromagnetically shielded, the noise level of the recorded data was comparable to that in the shielded space, indicating that our wireless recording system could be useful not only in indoor but also in outdoor experiments.

## Discussion

Cables between animals and recording devices are sometimes troublesome for studying behaviors, such as vocal communication in common marmosets<sup>16,31</sup>, perception of three-dimensional space in flying bats<sup>32</sup>, and burrowing behavior in rodents<sup>18</sup>. To overcome the difficulties, different types of wireless chronic recording systems have been developed<sup>16,18,31,32</sup>. Most of these wireless devices are designed to be used in combination with multi-channel recording electrodes

such as multi-electrode arrays, silicon probes, or tetrodes. However, these multi-channel recording approaches for studying single neuronal activity may not be suitable in some situations, such as when small brain areas are targeted, for example, or when a specific type of neuron, particularly with a small cell body or with a high firing rate, is studied<sup>4,8,12</sup>. To complement these approaches, we established a wireless recording method with a motorized microdrive. Using our system, the position of electrodes can be wirelessly adjusted with the micrometer precision (Fig. 1) so that activity of single neurons can be efficiently explored without affecting animal behavior (Fig. 4). Because the recorded data were transmitted using digital technology, our wireless system is robust to noise and allows high-quality recording comparable to the tethered recording system (Fig. 3). In addition, because the signals detected by the electrodes can be continuously monitored in real time, further strict analyses of single neuronal activity can be achieved by online or offline spike sorting.

When using such a wireless recording system with motorized positioners for electrodes, in exchange for being released from the restraints of cables, the subject must instead be loaded with all of the devices: a motor driver, an electrophysiological amplifier, and a wireless transceiver. We therefore developed a compact and lightweight WIF that integrates all of these devices (Fig. 1). One of the difficulties in constructing such a WIF is that it handles quite different types of electrical signals. The motor driver must synthesize voltage pulses with amplitude of 6 V generating currents of approximately 100 mA. In contrast, the electrophysiological amplifier must magnify faint neuronal signals under 100 microvolts. And the wireless transceiver not only continuously relays the recorded data from the amplifier to a remote computer but also intermittently relays the control commands from the computer to the motor driver. To implement these different functions through a compact WIF package, we utilized the MCU-based digital operation and a wireless technology termed Bluetooth. As a result, the WIF became small and light enough to be mountable on a rat's head, along with the motorized microdrive (Fig. 1g).

In addition to remote fine control of electrode positioning, the development of a compact wireless recording system for single-unit recording must address the problem of secure and high-speed transmission of the whole data. Although spike sorting is useful and widely used in various *in vivo* electrophysiological studies, the sorting analysis requires several processes, and subtle changes in each process dramatically affect the results<sup>9,10,33–35</sup>. Therefore, to determine the best spike-sorting algorithms suitable for each recording session, the whole recorded data should be transferred and stored in advance. Moreover, as shown in Figure 4b, a fine movement of a recording electrode greatly affects the intensity of neuronal signals and the isolation of single units from others or background noise. A rapid movement of the subject may cause the displacement of electrodes, resulting in an alteration of the signal condition. Therefore, ideally, the neuronal signal should be transmitted without interruption and observed in real time. As demonstrated in Figure 2b, the transfer rate of Bluetooth decreases with increasing distance. Therefore, for secure wireless transmission and real-time inspection of the data, one solution is to reduce the data size without losing the data quality before wireless transmission, and to restore the compressed data after receiving it. Thus, we created a simple and practical encoding program for reversible data compression. We optimized the encoding program based upon the characteristics of extracellularly recorded neuronal signals in different brain areas, which were digitized with a sampling frequency of 20 kHz and a 10-bit resolution; we added the first-order difference operation before the variable-length encoding process, and determined the compression parameter from a remote host computer. As a result, we successfully reduced the data size nearly to the theoretical boundary of lossless compression, which can be calculated as Shannon entropy<sup>27</sup>. The optimization of the

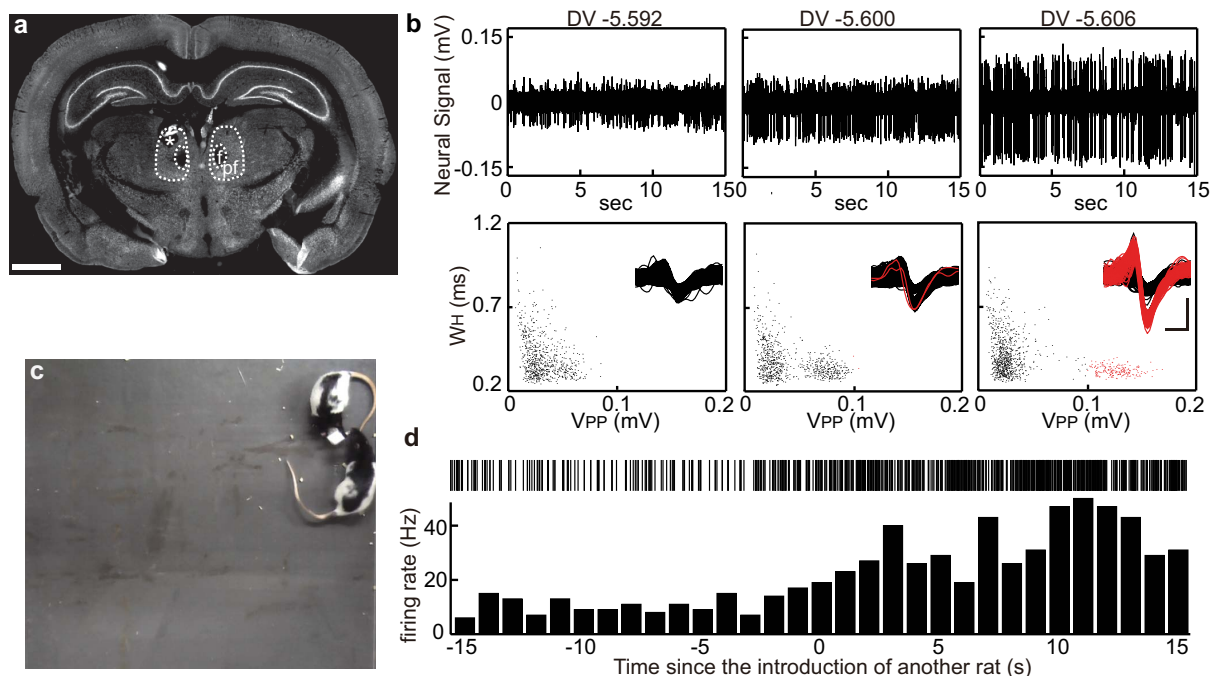


**Figure 4 | Wireless isolation and recording of single unit activity in the parafascicular nucleus from a freely behaving rat.** (a) A coronal section confirming the recording site (asterisk) in the parafascicular nucleus (PF). The sample was counter-immunostained with anti-NeuN antibody. Scale bar indicates 2 mm. f, fasciculus retroflexus. (b) Neural data recorded by the same electrode in the PF at a depth of 5.592 mm, 5.600 mm, and 5.606 mm are presented. For the scatter plot of spike width ( $W_H$ ) and spike peak amplitude ( $V_{PP}$ ), all deflections with a negative peak below  $-20 \mu\text{V}$  from the same data presented above were used. Overlaid waveforms of all the detected deflections including background noise are shown in the insets. Vertical and horizontal scale bars indicate  $100 \mu\text{V}$  and  $0.5 \text{ ms}$ , respectively. Black and red indicate deflections with a  $V_{PP}$  value  $< 0.1 \text{ mV}$  and  $\geq 0.1 \text{ mV}$ , respectively. (c) Another rat was introduced to the field. (d) Activity of a putative PF neuron in response to the introduction of another rat.

variable-length encoding process may depend on various factors, such as the gain and the filter properties of electrophysiological amplifiers and the sampling rate and the resolution of the analog-to-digital conversion process. For example, with a higher sampling

rate, a second- or third-order difference operation could more efficiently reduce the data size. Hence, to apply our encoding strategy to different brain areas or different recording setups, it is important to systematically examine the order of the difference operation and the compression parameter (Supplementary Fig. S3 and S4).

We demonstrated that single neuronal activity in a freely behaving rat could be wirelessly isolated and the recording system is less likely to interfere with its social interaction or communication than a wired device (Fig. 4). Such single-unit recordings during interactive behavior between two animals can also be performed using a tethered recording system<sup>12</sup>. However, our wireless system would allow electrophysiological study of behavior among a large number of animals. Furthermore, because the individual Bluetooth devices are designed to avoid interfering with each other by continuously changing the frequency for wireless communication using a radio technology called frequency-hopping spread spectrum, we can perform neural recording simultaneously from several different animals in the same place. Thus our wireless recording system with a motorized microdrive is useful for studying brain mechanisms involved in various social behaviors. Another advantage of our system is its portability and usability. Conventional tethered recording generally requires electrophysiological devices, power supplies for them, and electromagnetic shields. But, in some situations, it may be difficult to set up these apparatuses in large or outdoor spaces. In contrast, our wireless recording system works only with a battery-operated laptop computer equipped with a Bluetooth transceiver, and does not require any other devices that are necessary for analog systems<sup>16–19,31,32</sup>. One of the concerns about our recording system is its relative narrow working area in comparison with a previously reported analogue wireless recording system<sup>18</sup>. The wireless transmission range can be improved by selecting a Bluetooth transceiver with a high-performance antenna and adjusting its placement. Importantly, digital wireless communication such as Bluetooth technology, which is

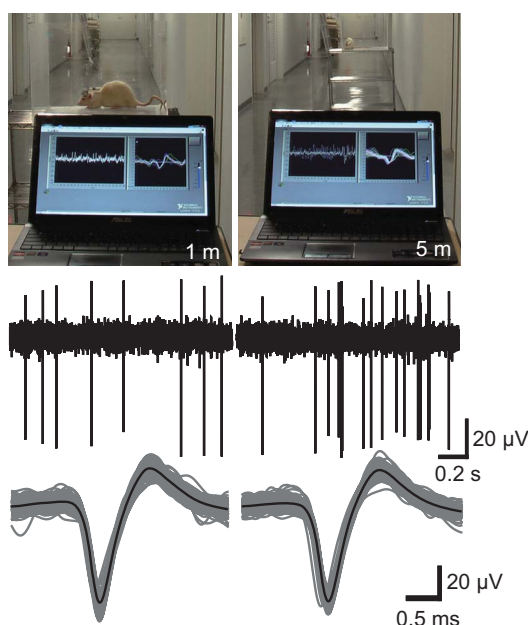


**Figure 5 | Wireless recording in an indoor open space.** Wireless recording of single neuronal activity in the thalamus was performed using a battery-operated laptop computer with a USB Bluetooth transceiver placed 1 m (left) or 5 m (right) from the animal. The space was not electromagnetically shielded.



broadly used in indoor or outdoor spaces, is highly resistant to noise and in general does not require any electro-magnetic shielding covering the space.

The wireless recording system reported here still has several limitations. For example, the wireless transmission rate of Bluetooth technology is lower than that necessary for simultaneous multichannel recording. The total weight of our system, especially a battery for the WIF, is still too heavy for behavioral studies of small animals such as mice and songbirds. However, our novel technologies for wireless recording, the wireless control system for electrode placement, and the lossless data-encoding system suitable for continuous monitoring and spike sorting analysis, can be further refined for more advanced neural recording systems in the future. The recording system reported here, or further improved devices, with the capability for wireless measurement of single neuronal activity in freely behaving animals, will open new possibilities in neuroscience research.

## Methods

**Motorized microdrive and wireless interface (WIF).** A miniature motorized microdrive was constructed as previously reported<sup>13</sup>, with minor modifications. The microdrive was equipped with custom-made planetary-gear BLDCs (reduction ratio, 1:337; Namiki Precision Jewel), and recording electrodes were fixed on the electrode-holding shuttles that could travel along the threaded motor shafts (pitch, 125  $\mu\text{m}$ ). The electrodes and the BLDC-terminals of the microdrive were connected to the WIF using a 10-pin male connector (Omnetics) cable. To minimize the artifacts and electromagnetic noise, we modified the cable and added buffer amplifiers for impedance matching between the 10-pin male connector of the microdrive side and the cable.

The WIF consisting of a motor driver for three BLDCs, a 3-channel electrophysiological amplifier, a Bluetooth transceiver, a power-supply circuit, and a MCU (LPC2368, NXP semiconductor) was assembled on a custom printed circuit board (Kansai Electronics). The core of the motor driver consists of CMOS analog-switch modules (MAX4602EAE, Maxim Integrated Products), each of which contains 4 normally-open type switches. The analog-switches are operated by the MCU through its GPIO ports. To estimate the minimal step distance of the electrode movement, the microdrive was placed on the stage of an inverted microscope (IX73, Olympus), and the electrode tip was imaged using a 20 $\times$  objective and CCD camera (DP80, Olympus). After generating the same command voltage signals (1 to 24 square pulses) 10 times, the total displacement of the electrode tip was measured using imaging software (cellSens Standard, Olympus). The electrophysiological amplifier, with a fixed gain of 5000, consists of two-stage operational amplifiers and fixed bandpass filter circuits (0.1–3 kHz), and its outputs were connected to the MCU ports for analog-to-digital conversion (measurement range, 0 V to +3 V). The Bluetooth transceiver (ZEAL-C02, ADC technologies) communicates with the MCU through the universal asynchronous receiver/transmitter (UART) ports. Thus the MCU relays the amplified neural signals to the Bluetooth transceiver and operates the BLDCs according to the motor commands received by the Bluetooth transceiver. Firmware, including a data-encoding program, for the MCU was written in C language.

**Animal preparation and implantation surgery.** All procedures were in accordance with the National Institutes of Health *Guide for the Care and Use of Laboratory Animals* and were approved by the Institutional Animal Care and Use Committee of Kyoto University.

Male Long-Evans rats (Institute for Animal Reproduction) weighing 450–550 g were used for the wireless recording experiments in freely behaving states and the operant conditioning (Supplementary Fig. S2). For other experiments, male Wistar rats (SLC) were used. Animals were kept under a 12:12 hr light:dark cycle with food and water *ad libitum*, except for those used for the operant conditioning in which water was removed 16–18 hr before the sessions during the experimental days.

Animals were initially anesthetized with an intraperitoneal administration of ketamine (50 mg/kg) and xylazine (2 mg/kg). After a skin incision, 10 miniature anchor screws were attached to the skull. A small hole was made in the skull above the area of interest, and the microdrive was positioned with the help of a stereotaxic apparatus. The stereotaxic coordinates from the bregma were as follows: anterior-posterior (AP) -4.0 mm, medial-lateral (ML) 1.0 mm (for recording in the PF) and AP -3.5– -4.0 mm, ML 2.3–2.5 mm (for recording in the cortex, thalamus, and hippocampus). After penetration of electrodes across the dura was confirmed, the microdrive was fixed on the skull with acrylic resin. The brain surface was protected with gentamicin-containing ointment. The WIF, sealed with epoxy-based glue to prevent short circuits, was fixed on the head along with the microdrive.

To power the WIF, we used lithium-ion rechargeable batteries (3.7 V, 160 mAh, 4.0 g, 39  $\times$  12  $\times$  8 mm, Turnigy nano-tech). A single battery, or 4 batteries connected in parallel, was carried using a jacket harness (RJ02, BRC). For operant training, we used 4 batteries (total weight 16.0 g). We could conduct continuous recording for 3 hours using 4 batteries and for 1 hour using a single one. The electric power required for driving the BLDCs is approximately 400 mW, which is almost twice as much as that for wireless transmission. However, each operation of the BLDCs is

instantaneous (20–100 ms) and control of the electrode position did not affect battery lifetime.

**Histological analysis.** After electrophysiological recordings, rats were deeply anesthetized with an overdose of sodium pentobarbital (100 mg/kg, i.p.). Marking lesions were made by passing DC currents (10  $\mu\text{A}$  for 20 s) through recording electrodes as previously described<sup>13</sup>. Animals were perfused transcardially with 4% formaldehyde in 0.1 M phosphate buffer (PB), pH 7.3. Brain samples were cryoprotected with 30% sucrose in PBS overnight at 4°C, and cryosectioned coronally into 40- $\mu\text{m}$ -thick sections. After pre-incubation with PBS containing 10% normal goat serum and 0.1% Triton X-100, the sections were incubated with mouse anti-NeuN antibody (1:1000; MAB377, Millipore) in PBS containing 10% normal goat serum and 0.1% Triton X-100 overnight at 4°C. After washes in PBS, the sections were incubated with goat anti-mouse immunoglobulin G conjugated with Alexa 488 (1:500; A11029, Invitrogen) for 1 hr at room temperature. All sections were imaged using a fluorescence microscope (BZ-9000, Keyence). Images were acquired with a 4 $\times$  objective and tiled together using a BZ-II Analyzer to show the whole section images.

**Wireless and wired recording and data acquisition.** For all the recording sessions, tungsten electrodes with 1.2–1.5 M $\Omega$  impedance at 1 kHz (MicroProbes) were used. For wireless recording through the WIF, a desktop or laptop computer running under Microsoft Windows 7 (64-bit) with a USB Bluetooth dongle (BT-MicroEDR2X, Planex Communications Inc.) was used. The data transmitted through the Bluetooth wireless transceiver on the subject were decoded by a custom program running as a dynamic link library under Windows OS. For tethered recording, recording electrodes were connected to the head stage (H2P, Grass Technologies) of an electrophysiological amplifier (P511, Grass Technologies). The data obtained by the tethered system were bandpass-filtered (0.1–3 kHz) and analog-to-digital converted with a sampling frequency of 20 kHz using a data acquisition card (PCI-6052E, National Instruments).

**Data analysis.** Offline spike sorting and all statistical analyses were conducted using MATLAB. Offline spike sorting was performed in a semi-automated manner. All negative peaks with amplitude above a manually defined peak threshold were extracted. Then, waveforms around the negative peaks were used to calculate peak-to-peak voltages ( $V_{PP}$ ) and widths of the half trough ( $W_H$ ).  $V_{PP}$  was defined as the amplitude difference of the negative peak to the maximum value within 1 ms.  $W_H$  was defined as the difference in time between the two sample points crossing the 50% mark of the negative peak amplitude. Then, the scatter plot of  $W_H$  and  $V_{PP}$  was generated and spike events were manually clustered.

Signal-to-noise ratio (SNR) was defined by the equation below, as previously described<sup>16</sup>:

$$\text{SNR} = 20 \log_{10} \frac{V_{PP}}{\text{SD}_N} \quad (1)$$

where  $\text{SD}_N$  indicates the standard deviation of the background noise (0.3–0.6 ms preceding all negative peaks).

Entropy of neural signals before and after the first-, second-, or third-order difference operation was calculated to assess the theoretical limit for reversible compression, because it is impossible to compress the data to less than the source entropy (information-theoretic content)<sup>27</sup>. Given a neural signal  $X$  with integers ranging from -1023 to 1023, the Shannon's information amount for value  $i$ ,  $I(i)$ , and entropy,  $H$ , were calculated as follows:

$$I(i) \equiv \begin{cases} 0, & \text{if } P(i) = 0 \\ -\log_2 P(i), & \text{otherwise} \end{cases} \quad (2)$$

$$H(X) \equiv - \sum_{i=-1023}^{1023} P(i) I(i) \quad (3)$$

where  $P(i)$  is the fraction (or probability) of value  $i$  within  $X$ . With a base 2 logarithm as shown above, both information amount and entropy have "bit" as units.

- Hubel, D. H. & Wiesel, T. N. Receptive fields, binocular interaction and functional architecture in the cat's visual cortex. *J. Physiol. (Lond.)* **160**, 106–154 (1962).
- Wilson, M. A. & McNaughton, B. L. Dynamics of the hippocampal ensemble code for space. *Science* **261**, 1055–1058 (1993).
- Winson, J. A compact micro-electrode assembly for recording from the freely-moving rat. *Electroencephalogr Clin Neurophysiol* **35**, 215–217 (1973).
- McNaughton, B. L., O'Keefe, J. & Barnes, C. A. The stereotrode: a new technique for simultaneous isolation of several single units in the central nervous system from multiple unit records. *J. Neurosci. Methods* **8**, 391–397 (1983).
- Bragin, A. *et al.* Multiple site silicon-based probes for chronic recordings in freely moving rats: implantation, recording and histological verification. *J. Neurosci. Methods* **98**, 77–82 (2000).
- Costa, R. M., Cohen, D. & Nicolelis, M. A. L. Differential corticostriatal plasticity during fast and slow motor skill learning in mice. *Curr. Biol.* **14**, 1124–1134 (2004).



7. Hubel, D. H. Single unit activity in striate cortex of unrestrained cats. *J. Physiol. (Lond.)* **147**, 226–238 (1959).
8. Fee, M. S. & Leonardo, A. Miniature motorized microdrive and commutator system for chronic neural recording in small animals. *J. Neurosci. Methods* **112**, 83–94 (2001).
9. Lewicki, M. S. A review of methods for spike sorting: the detection and classification of neural action potentials. *Network* **9**, R53–78 (1998).
10. Quiroga, R. Q. Spike sorting. *Curr. Biol.* **22**, R45–6 (2012).
11. Hahnloser, R. H. R., Kozhevnikov, A. A. & Fee, M. S. An ultra-sparse code underlies the generation of neural sequences in a songbird. *Nature* **419**, 65–70 (2002).
12. Luo, M., Fee, M. S. & Katz, L. C. Encoding pheromonal signals in the accessory olfactory bulb of behaving mice. *Science* **299**, 1196–1201 (2003).
13. Fujimoto, H., Hasegawa, T. & Watanabe, D. Neural coding of syntactic structure in learned vocalizations in the songbird. *J. Neurosci.* **31**, 10023–10033 (2011).
14. Prather, J. F., Peters, S., Nowicki, S. & Mooney, R. Precise auditory-vocal mirroring in neurons for learned vocal communication. *Nature* **451**, 305–310 (2008).
15. Prather, J. F., Nowicki, S., Anderson, R. C., Peters, S. & Mooney, R. Neural correlates of categorical perception in learned vocal communication. *Nat. Neurosci.* **12**, 221–228 (2009).
16. Roy, S. & Wang, X. Wireless multi-channel single unit recording in freely moving and vocalizing primates. *J. Neurosci. Methods* **203**, 28–40 (2012).
17. Schregardus, D. S. *et al.* A lightweight telemetry system for recording neuronal activity in freely behaving small animals. *J. Neurosci. Methods* **155**, 62–71 (2006).
18. Szuts, T. A. *et al.* A wireless multi-channel neural amplifier for freely moving animals. *Nat. Neurosci.* **14**, 263–269 (2011).
19. Ruther, P. *et al.* Compact wireless neural recording system for small animals using silicon-based probe arrays. *Conf Proc IEEE Eng Med Biol Soc* **2011**, 2284–2287 (2011).
20. Hampson, R. E., Collins, V. & Deadwyler, S. A. A wireless recording system that utilizes Bluetooth technology to transmit neural activity in freely moving animals. *J. Neurosci. Methods* **182**, 195–204 (2009).
21. Aceros, J., Yin, M., Borton, D. A., Patterson, W. R. & Nurmikko, A. V. A 32-channel fully implantable wireless neurosensor for simultaneous recording from two cortical regions. *Conf Proc IEEE Eng Med Biol Soc* **2011**, 2300–2306 (2011).
22. Thomas, S. J., Harrison, R. R., Leonardo, A. & Reynolds, M. S. A battery-free multichannel digital neural/EMG telemetry system for flying insects. *IEEE Trans Biomed Circuits Syst* **6**, 424–436 (2012).
23. Ball, D. *et al.* Rodent scope: a user-configurable digital wireless telemetry system for freely behaving animals. *PLoS ONE* **9**, e89949 (2014).
24. Minamimoto, T., Hori, Y. & Kimura, M. Roles of the thalamic CM-PF complex-Basal ganglia circuit in externally driven rebias of action. *Brain Res. Bull.* **78**, 75–79 (2009).
25. Smith, Y. *et al.* The thalamostriatal systems: anatomical and functional organization in normal and parkinsonian states. *Brain Res. Bull.* **78**, 60–68 (2009).
26. Smith, Y., Surmeier, D. J., Redgrave, P. & Kimura, M. Thalamic contributions to Basal Ganglia-related behavioral switching and reinforcement. *J. Neurosci.* **31**, 16102–16106 (2011).
27. MacKay, D. J. C. [Symbol Codes] *Information Theory, Inference and Learning Algorithms* [90–108] (Cambridge University Press, Cambridge, 2003).
28. Van der Werf, Y. D., Witter, M. P. & Groenewegen, H. J. The intralaminar and midline nuclei of the thalamus. Anatomical and functional evidence for participation in processes of arousal and awareness. *Brain Res. Brain Res. Rev.* **39**, 107–140 (2002).
29. Minamimoto, T., Hori, Y. & Kimura, M. Complementary process to response bias in the centromedian nucleus of the thalamus. *Science* **308**, 1798–1801 (2005).
30. Brown, H. D., Baker, P. M. & Ragozzino, M. E. The parafascicular thalamic nucleus concomitantly influences behavioral flexibility and dorsomedial striatal acetylcholine output in rats. *J. Neurosci.* **30**, 14390–14398 (2010).
31. Hage, S. R., Jürgens, U. & Ehret, G. Audio-vocal interaction in the pontine brainstem during self-initiated vocalization in the squirrel monkey. *Eur. J. Neurosci.* **23**, 3297–3308 (2006).
32. Yartsev, M. M. & Ulanovsky, N. Representation of three-dimensional space in the hippocampus of flying bats. *Science* **340**, 367–372 (2013).
33. Harris, K. D., Henze, D. A., Csicsvari, J., Hirase, H. & Buzsáki, G. Accuracy of tetrode spike separation as determined by simultaneous intracellular and extracellular measurements. *J. Neurophysiol.* **84**, 401–414 (2000).
34. Quiroga, R. Q., Nadasdy, Z. & Ben-Shaul, Y. Unsupervised spike detection and sorting with wavelets and superparamagnetic clustering. *Neural Comput* **16**, 1661–1687 (2004).
35. Rutishauser, U., Schuman, E. M. & Mamelak, A. N. Online detection and sorting of extracellularly recorded action potentials in human medial temporal lobe recordings, in vivo. *J. Neurosci. Methods* **154**, 204–224 (2006).

## Acknowledgments

We thank Drs. Y. Sakurai and K. Hamaguchi for helpful comments, and Dr. J.A. Hejna for careful reading of the manuscript and invaluable advice. This work was supported by research grants from the Takeda Science Foundation, and the Ministry of Education, Culture, Sports, Science, and Technology of Japan including the Strategic Research Program for Brain Sciences and Grant-in-Aid for Scientific Research (24220009).

## Author contributions

T.H. carried out all of the experiments; H.F., K.T., M.N., and A.T. helped with some experiments; T.H. and D.W. wrote the paper.

## Additional information

**Supplementary information** accompanies this paper at <http://www.nature.com/scientificreports>

**Competing financial interests:** The authors declare no competing financial interests.

**How to cite this article:** Hasegawa, T. *et al.* A wireless neural recording system with a precision motorized microdrive for freely behaving animals. *Sci. Rep.* **5**, 7853; DOI:10.1038/srep07853 (2015).



This work is licensed under a Creative Commons Attribution-NonCommercial-ShareAlike 4.0 International License. The images or other third party material in this article are included in the article's Creative Commons license, unless indicated otherwise in the credit line; if the material is not included under the Creative Commons license, users will need to obtain permission from the license holder in order to reproduce the material. To view a copy of this license, visit <http://creativecommons.org/licenses/by-nc-sa/4.0/>